Journal of Medicinal Chemistry

Article

Conformation-Based Restrictions and Scaffold Replacements in the Design of HCV Polymerase Inhibitors: Discovery of Deleobuvir (BI 207127)

Steven R. LaPlante, Michael Bos, Christian Brochu, Catherine Chabot, René Coulombe, James R. Gillard, Araz Jakalian, Martin Poirier, Jean Rancourt, Timothy Stammers, Bounkham Thavonekham, Pierre L. Beaulieu, George Kukolj, and Youla S. Tsantrizos

J. Med. Chem., **Just Accepted Manuscript** • Publication Date (Web): 25 Oct 2013

Just Accepted

Journal of Medicinal Chemistry is published by the American Chemical Society. 1155 Sixteenth Street N.W., Washington, DC 20036

Conformation-Based Restrictions and Scaffold Replacements in the Design of HCV Polymerase Inhibitors: Discovery of Deleobuvir (BI 207127)

Steven R. LaPlante,[‡]* Michael Bös, Christian Brochu, Catherine Chabot, René Coulombe, James R. Gillard, Araz Jakalian, Martin Poirier, Jean Rancourt, Timothy Stammers, Bounkham Thavonekham, Pierre L. Beaulieu, George Kukolj, Youla S. Tsantrizos[‡]*

Departments of Chemistry and Biological Sciences, Boehringer Ingelheim (Canada) Ltd., 2100 Cunard Street, Laval (Quebec) Canada, H7S 2G5

ABSTRACT

Conformational restrictions of flexible torsion angles were used to guide the identification of new chemotypes of HCV NS5B inhibitors. Sites for rigidifications were based on an acquired conformational understanding of compound binding requirements and the roles of substituents in the free and bound states. Chemical bioisosteres of amide bonds were explored in order to improve cell-based potency. Examples are shown, including the design concept that led to the discovery of the phase III clinical candidate deleobuvir (BI 207127). The structure-based strategies employed have general utility in drug design.

INTRODUCTION

The optimization and exploitation of ligand binding to macromolecules, which is one of the primary goals of medicinal chemistry, may often be confounded by a variety of interrelated factors. Structure-activity relationships attempt to elucidate the importance and impact of direct ligand-protein interactions such as van der Waals surface contacts, lipophilic and ionic attractions as well as the establishment of hydrogen bonds and solvation influences.[1] However, there are some other less characterized but nonetheless important factors. These include, but are not limited to, conformational changes associated with the binding events (ligand and protein). The deconvolution of the individual enthalpic and entropic energy components detailed above often prove to be very challenging or seemingly impossible. While significant advances have led to receptor induced-fit and conformational selection models that describe bimolecular

recognition,[1,2] a more comprehensive view of the impact of shape and conformational changes upon binding are still evolving.[3-5] Ligand-receptor association may be viewed as the collision of two flexible objects where their transient shapes must have sufficient complementarities to enable initial contact followed by mutual adaptations to stabilize the interactions. Deciphering the precise details of the collision and binding events remains largely elusive and impractical in drug discovery, but if trends are exposed and properly exploited, then breakthroughs may be possible.[3]

This work describes our approach in acquiring information about the ligand shape and conformational changes associated with the binding events, from which rigidification proposals and analogues were then generated as a mean of exploring new chemotypes and chemically diverse series of compounds. The examples discussed here involve targeting the thumb pocket 1 allosteric site of the NS5B polymerase of the hepatitis C virus (HCV).[6]

RESULTS AND DISCUSSION

Our initial HCV NS5B polymerase hit (compound **1**; Figure 1) came from a high-throughput screen of our compound collection.[7] Ligand-based optimization led to the potent tryptophan-benzimidazole analog **2**,[7b,h] but this series lacked many desired properties for an effective anti-HCV drug (e.g. cell culture activity) presumably due to the effects of two ionizable carboxylic acid functions. A knowledge-based strategy successfully "linker hopped" to a new structural hinge that led to a promising diamide chemical series (e.g. compound **3**; Figure 1) that appropriately matched the ligand bioactive conformation and pocket bioactive space.[3,7f] Subsequently, hit-to-lead and lead

optimization[8a] efforts led to several structural modifications, including the replacement of the benzimidazole scaffold with the more lipophilic indole isostere, and identification of BILB 1941 (compound **4**, Figure 1), which was advanced to clinical development. This compound was the first inhibitor of HCV NS5B binding to the thumb pocket I allosteric site to demonstrate proof-of-concept in reducing viral load in patients infected with HCV genotype-1, albeit with limited potency at the tolerated doses.[8]

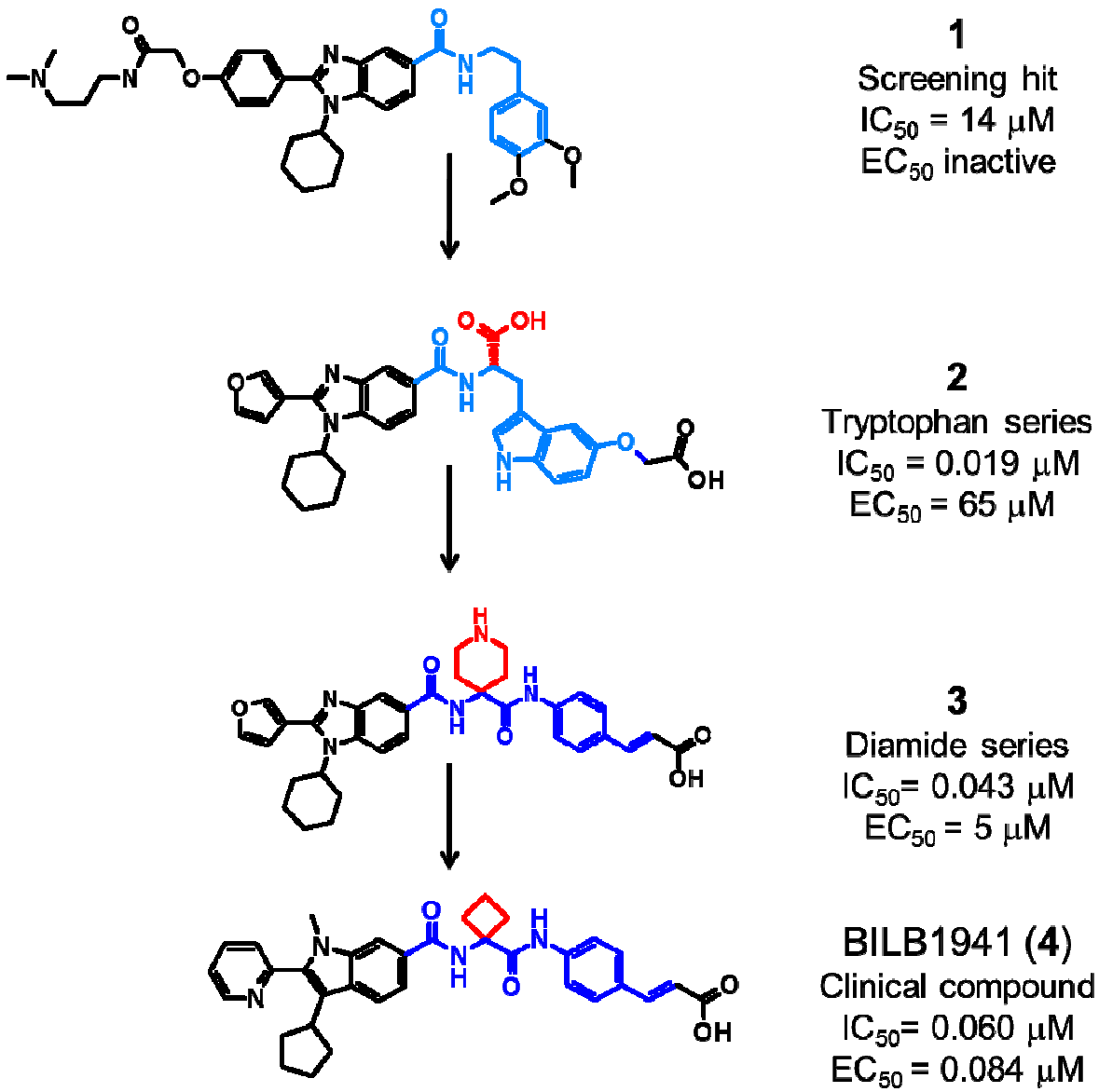

Figure 1. Key lead series discovered as thumb pocket 1 HCV polymerase inhibitors. Blue and red denotes those atoms involved in the structural hinge. For the IC_{50} assay, the Δ21 NS5B construct from GT-1b was used.[7g] For the EC_{50} assay, a GT-1b luciferase reporter assay was employed.[12,7e]

Efforts were then focused on identifying new series of compounds that bound to the same site and had improved cell-based potency and pharmacological properties. The rationale employed to transition to new and promising series was based on an acquired understanding of ligand binding requirements and substituent roles in the free and bound states of our initial leads.

An overview of our understanding of the roles of each substituent for **4** was assembled via multidisciplinary approaches and is summarized in Figure 2. The ensemble of information was consistent with the cyclopentyl ring playing an important role, as it binds in a lipophilic pocket exposed upon displacement of the Λ1 finger loop that interacts with the thumb domain in the apo state.[3] The pyridyl group lies over the protein surface and appears to have minor binding attributes as supported by the lack of NMR differential line broadening, and SAR studies that show that a plethora of substituent replacements are possible at this position.[3,7a-d,h,8a] This substituent's principal role is likely to help orient and sterically rigidify the free state of the critical cyclopentyl ring to adopt the bioactive conformation. The indole has an important scaffolding role, orienting the appendages along the α, β and γ torsion angles (Figure 2). This bicylic scaffold also lies perfectly flat against a receptor cliff. The methyl group helps rigidify the α torsion angle and may be involved in weak electrostatic interactions with the polymerase backbone carbonyls of Leu 492 and Gly 493.[3] The right-hand side of this

compound employs an α,α-disubstituted amino acid as a structural hinge that links with and enables the phenyl cinnamic acid right-hand side to lie flat over the upper receptor plateau. The carbonyl located between angles γ and δ is involved in a hydrogen-bond with Arg 503 (not highlighted in the surface display in Figure 2).

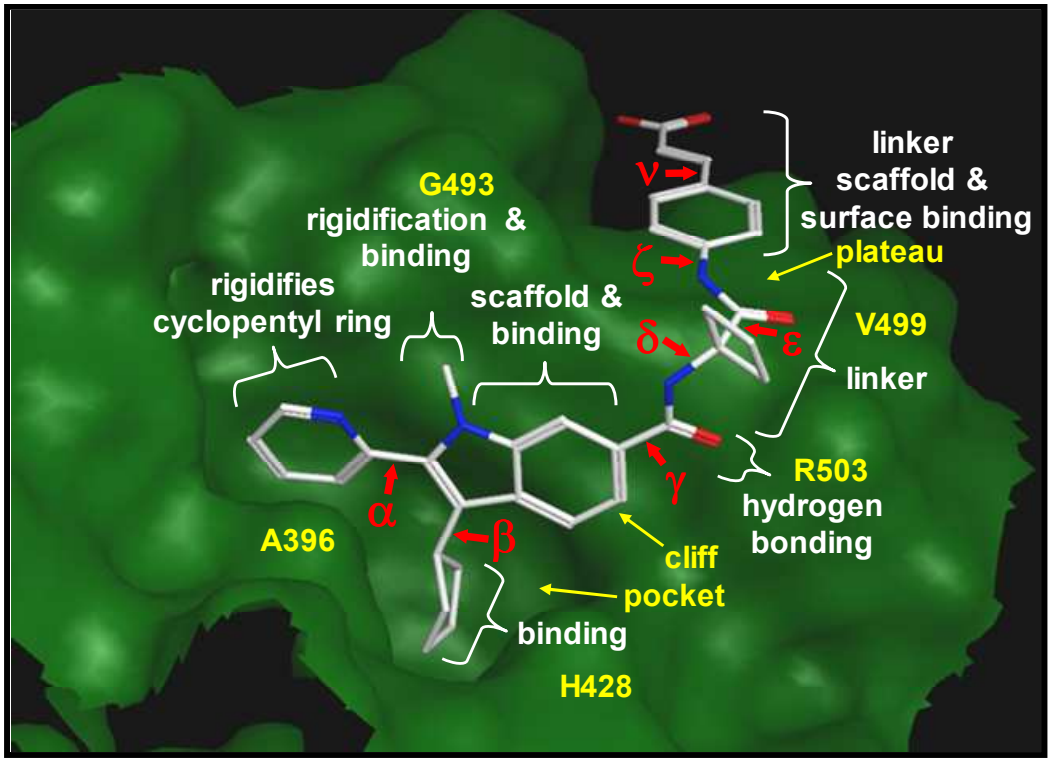

Figure 2. Shown is a model structure of **4** bound to thumb pocket 1 of HCV polymerase. The model shown was generated using a combination of X-ray structures of related compounds, NMR bound data, and docking.[3] Also displayed are interpretations of the roles of each substituent derived from multidisciplinary efforts. The red-colored Greek letters α-ν designate the torsion angles for which conformational restrictions were explored and discussed herein. Some amino acid residues and features of the HCV polymerase binding site are indicated in yellow.

Given the wealth of knowledge built around this diamide series as well as the earlier tryptophan analogues,[3,7,8] multiple ideas for conformational restrictions and scaffold replacements were proposed to identify new possible chemotypes. Studies

exemplified here involved the torsion angles designated by Greek letters (red) in Figure 2.

The first examples involving conformational rigidifications of the left-hand side were focused on torsion angles α and β. We reported earlier that an important role of the pyridyl group at the indole C-2 position was to sterically orient the critical cyclopentyl to its bioactive conformation.[7h] Thus, both substituents appeared to be conformationally interdependent through the rotation energy barriers for angles α and β.[7h] This was corroborated with the creative efforts of other groups by designing novel macrocycles of various ring sizes that attempt to rigidify the C-2 substituent in its bioactive conformation (as revealed by X-ray crystallography).[9]

Analogue **5** (Figure 3) provides a literature example of this type of "top cyclization" (red), and additional examples are shown in the Supporting Information.[9] This compound had impressive activity in cell culture (EC_{50} = 0.004 μM), and many new compounds have been discovered that apply similar and more elaborate "top cyclization" strategies. Other pharmaceutical companies have found that some analogs with "top cyclizations" had improved PK profiles, and compounds that are based on this concept are in clinical development.[9]

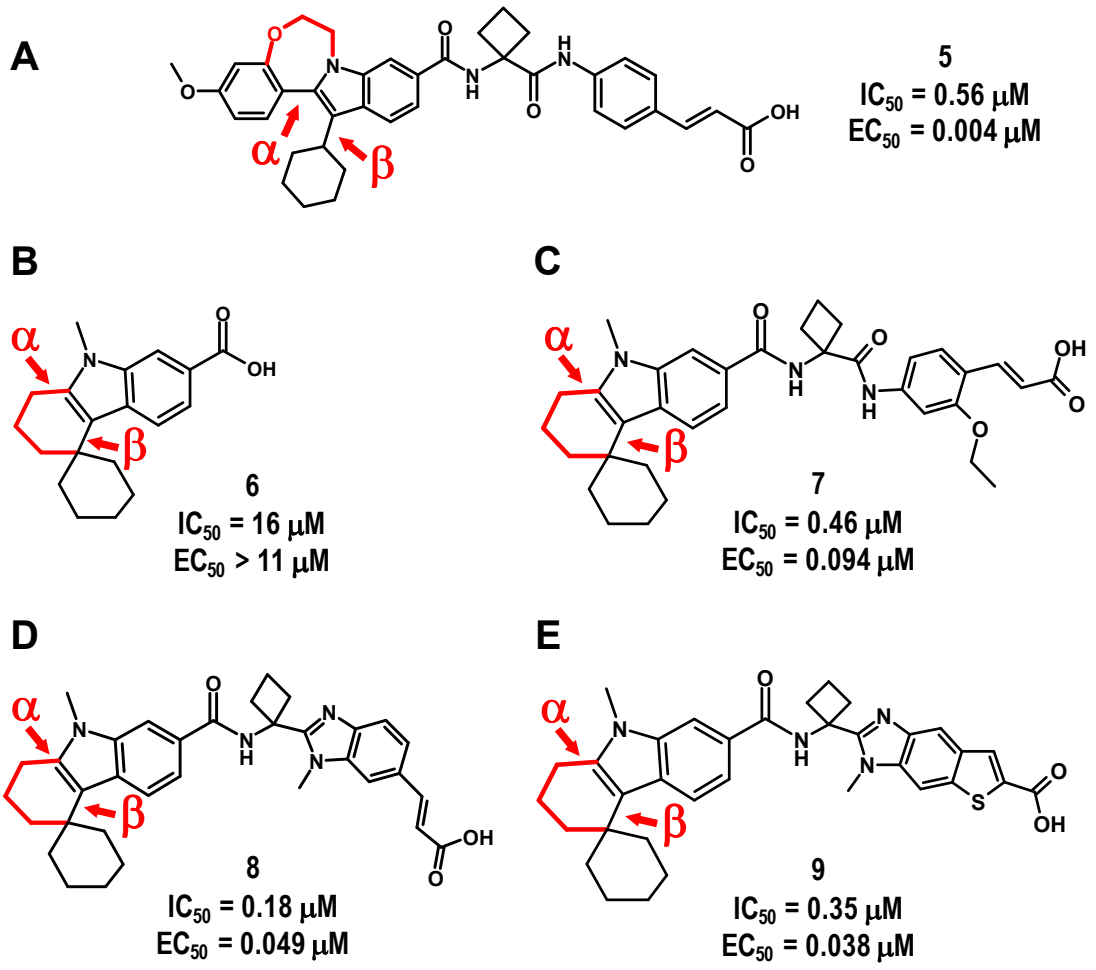

Figure 3. Example of conformational restrictions along torsion angles α and β (colored red). For the IC_{50} assay, the Δ21 NS5B construct from GT-1b was used.[7g] For the EC_{50} assay, a GT-1b luciferase reporter assay was employed.[12,7e]

We also applied "bottom cyclization" strategies to constrict rotations along both α and β torsion angles. Figure 3 provides examples of "bottom cyclizations" (colored red) as in compounds **6-9**. Compound **6** exhibited poor activity (80-fold drop in potency) compared to the corresponding unrestricted analogs bearing a heterocycle such as 2-pyridyl at C-2 (IC_{50} = 0.23 μM).[7c,h] Nonetheless, this type of cyclization, when combined with more optimal right-side groups that compensate for the loss in intrinsic potency of

the left-hand side, has the potential to provide alternate chemotypes with good cell culture activity as shown for compounds **7**, **8** and **9**.

In parallel to the above studies, chemical modifications were applied to restrict conformational flexibility along torsion angle γ (Figure 4). Studies were performed on a related benzimidazole series with improved solubility and amenable to biophysical analyses. Compound **10** exhibited ROESY NMR cross-peaks between amide hydrogen 1 and both aromatic hydrogens 16 and 18, implying conformational heterogeneity along γ in the free state. Earlier energy calculations reported low energy minima when the directly attached left-side amide and benzimidazole planes were mostly co-planar, suggesting that the amide can adopt two orientations - the bioactive "up orientation" where NH1 is close to 18 and the non-bioactive "down orientation" where NH1 is close to 16.[3,7h] Therefore, the above data were consistent with only half of the molecules adopting the bioactive "up orientation" along γ in the free state.

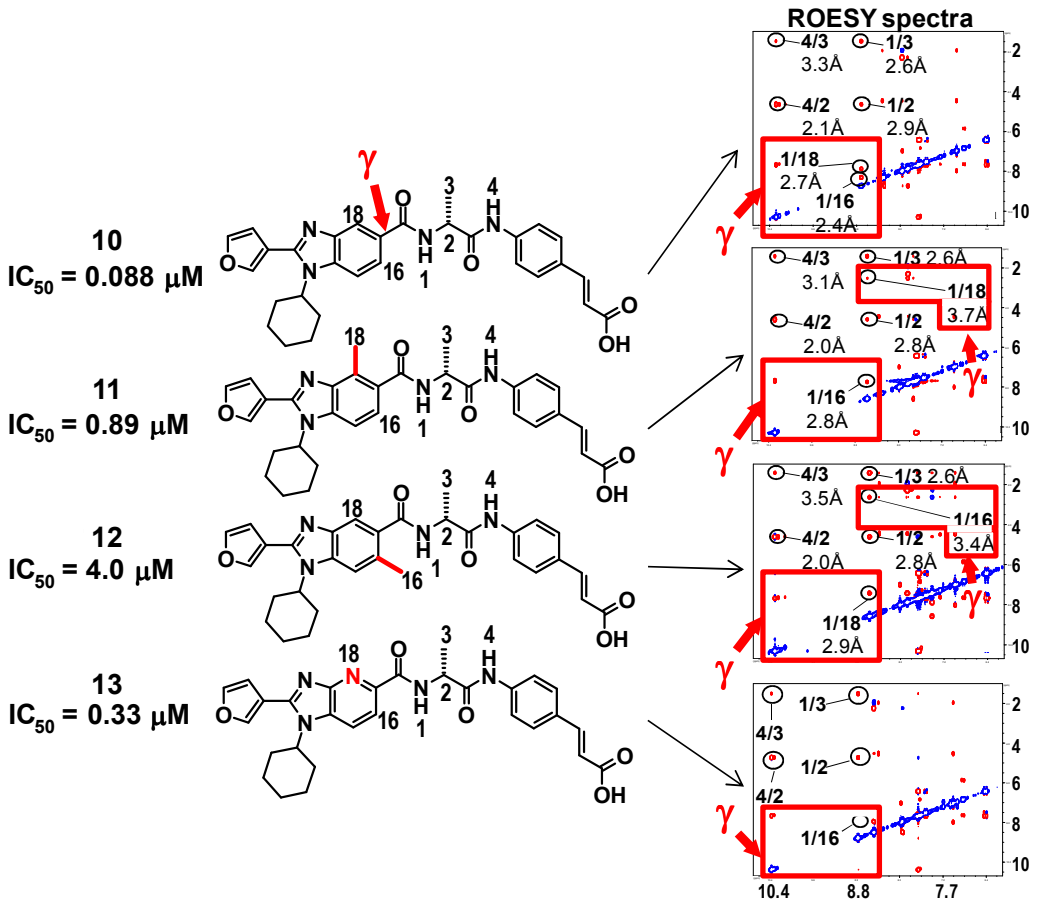

Figure 4. Shown are the structures and inhibition activities of methyl and aza analogues. NMR ROESY are shown for the compounds in the diamide series. ROESY data provide inter-hydrogen distance information for small molecules in the free-state, allowing the determination of conformational preferences in the free-state.

We therefore designed compounds **11** and **13** (Figure 4) with chemical modifications that were meant to promote the bioactive "up orientation" of the amide NH1. For compound **11**, it was envisioned that placing a methyl group at position 18 would result in a steric clash with the proximate amide carbonyl thus forcing the amide NH1 into or close to the bioactive "up orientation". As a control, compound **12** was also made with the methyl placed at position **16**. Unfortunately, compounds **11** and **12** were both much less potent than the unrestricted control compound **10**. Calculations suggested that this may be the result of distorting the amide plane away from the benzimidazole

plane,[7h] and ROESY NMR data on the right of Figure 4 are consistent with the methyl groups forcing a mix of conformations given that compounds **11** and **12** have peaks between the amide hydrogen 1 to both hydrogens 16 and 18. It is noteworthy that the carbonyl group of this amide bond is involved in a critical hydrogen bond with the guanidinium side chain of Arg 503 and disturbing the orientation of this group could have a negative impact on potency. Thus, methylation did not force a single amide orientation but rather allowed non-bioactive, free-state conformations as was also noted for the unsubstituted derivative **10**. Other factors could also have contributed to the loss in potency. For example, methylation at position 16 may have also introduced unfavorable steric clashes with the receptor pocket (e.g. compound **12**). However, this should not be the case for methylation at position 18 given that it should be solvent exposed in the bound state. More likely in this case, methylation distorts the amide away from the bioactive conformation. Given the above, it was concluded that methylated analogues had undesirable properties, and alternative strategies for rigidifying γ should be thought.

Calculations[7h] suggested that incorporation of nitrogen at position 18 would result in low energy minima such that amide NH1 would preferentially promote the bioactive "up orientation" of the amide (via the nitrogen lone pair electrons and the amide NH1). The corresponding aza-benzimidazole was made (compound **13**) and the expected free-state conformation was corroborated by NMR data, where no ROESY peak was observed between hydrogens 1 and 16 (bottom right of Figure 4); a result only possible if compound **13** adopted the lowest energy "up orientation" of the amide NH1. However, a comparison of the activities of the control compound **10** versus aza-benzimidazole **13** showed a 4-fold loss in potency, despite conformational rigidification toward the

bioactive conformation. It is likely that the loss in potency upon incorporating a nitrogen arose mainly from another unfavorable source, such as electrostatic incompatibility between the negative electrostatic potential introduced by incorporation of the nitrogen on the ligand with the negative electrostatic potential of the corresponding site of the receptor (see Supporting Information). Despite the fact that the nitrogen and methylation strategy described here failed to spawn attractive chemotypes, it did demonstrate that analysis tools, in particular NMR, may be used to better understand undesired and unexpected properties.

Conformational rigidification efforts were also directed to the extended diamide right-hand side of inhibitors. It was noteworthy that the potencies of analogs bearing a cinnamyl moiety in either meta or para position with respect to the aniline nitrogen were similar (unpublished data; refer also to the example in Appendix 3 of the Supporting Information). Consistent with this positional tolerability, the flexible ν torsion angle of the cinnamic acid moiety could be replaced with a variety of rigid and planar 5-membered rings (data not shown). One interesting example is shown in Figure 5A as compound **14**. This compound had attractive potency and solubility properties which made it amenable to NMR solution studies for better understanding its binding to the polymerase. NMR experiments were performed using differential line broadening (DLB) techniques[13] to differentiate the ligand substituents that contacted the receptor from those that were solvent exposed. This was done by superimposing the one-dimensional ^{1}H NMR spectra of free **14** (blue in Figure 5B) with that of **14** in the presence of HCV polymerase (red in Figure 5B). Ligand resonances that differed the most (see dotted

ovals in Figure 5B) are those that report contacts with the receptor, and those that do not change are assumed to be solvent exposed in the free and bound states.

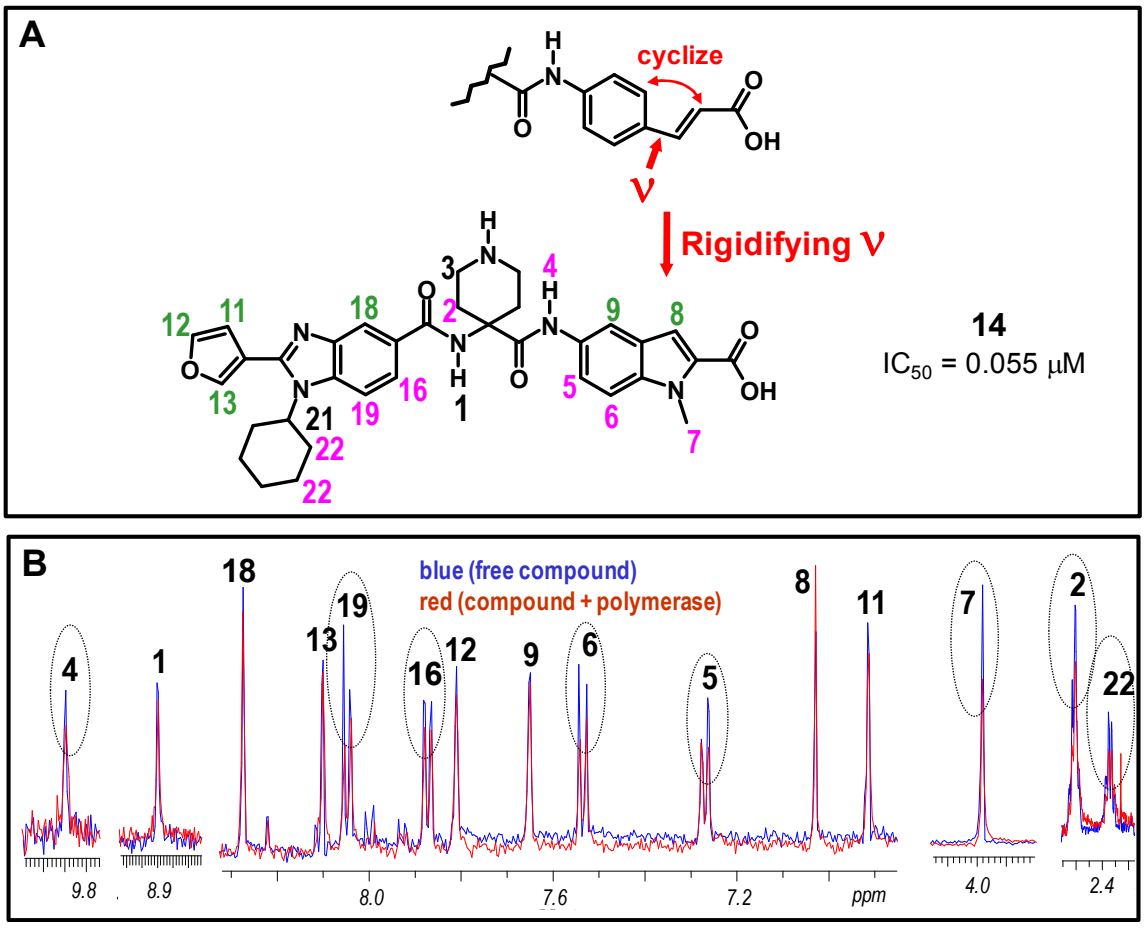

Figure 5. (A) The structure of compound **14** with the hydrogen nomenclature colored based on observed DLB data given in (B). Magenta numbers denote hydrogen resonances that changed significantly upon the addition of HCV polymerase; green numbers are hydrogens that experienced insignificant changes, and black numbers signify ambiguous data. (B) Blue ^{1}H NMR spectrum is of free **14** (at 200 μM), and the red spectrum is after adding HCV polymerase (at 20 μM).

The DLB data are summarized in Figure 5A where the hydrogen numbers are colored magenta for resonances which changed the most, and hydrogen numbers are colored green for those resonances that experienced little or no change. No conclusions

could be made for hydrogen numbers colored black. The ensemble of this DLB data suggested that the bottom part of **14** contacted the receptor (magenta numbers are all at the bottom), whereas the top part was solvent exposed (green numbers are at the top). Overall, the DLB data are consistent with compound binding in a similar manner as the related complex shown for **4** in Figure 2.

Attempts were then made to modulate the free state conformational properties by changing the position of the nitrogen of the central structural hinge as was described in detail for an earlier series.[3] However, Figure 6 showed that the related enantiomeric analogues **15** and **16** did not provide improved potencies. Nonetheless, all three compounds were then subjected to NMR transferred NOESY experiments[13] in the presence of the polymerase to determine the bound conformations using crosspeaks that report intra-ligand hydrogen distance information (<5Å) (Figure 6). Our intention was to identify a bound conformation that would be representative of the series. However, an analysis of the transferred NOESY data for all three compounds in Figure 6 suggested that the right side of these compounds did not adopt identical conformations; instead, they assumed alternate torsion angles along ζ and ε. For example, the relative crosspeak intensities between hydrogens 4/5 and between 4/9 are similar in Figure 6C and 6D but different in Figure 6B. Also, a crosspeak was observed between hydrogens 4/18 in Figure 6D, whereas it was lacking in 6B and 6C. Likewise, a crosspeak was noted between hydrogens 4/1 in Figure 6B, but lacking in 6C and 6D.

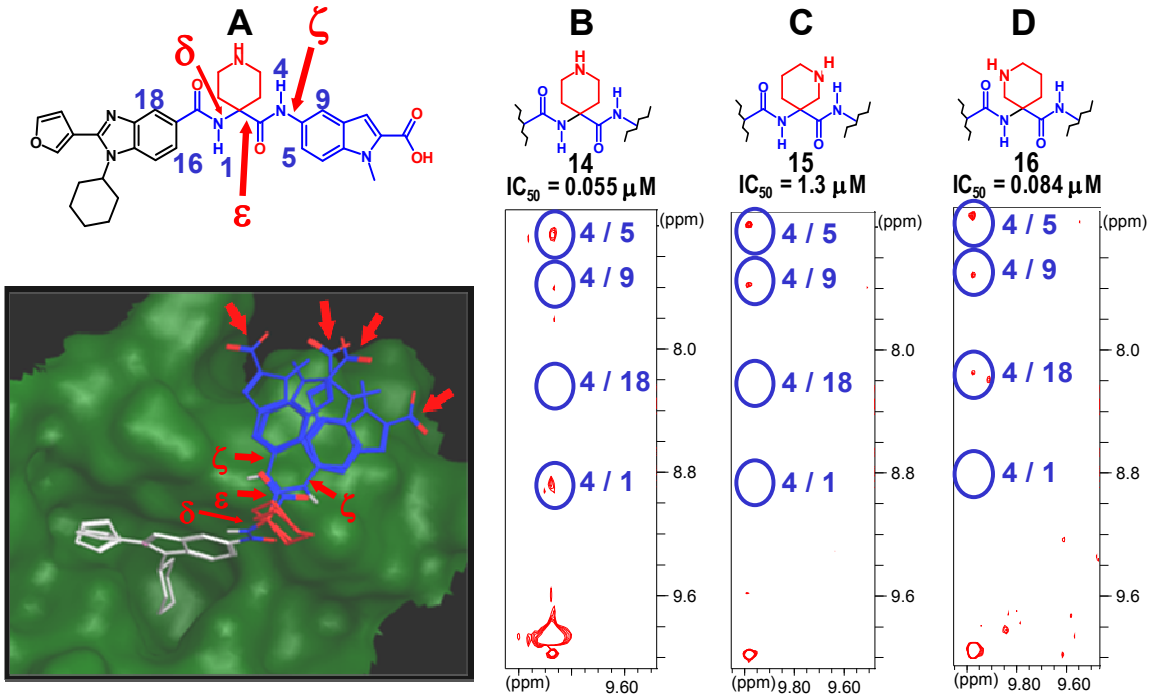

Figure 6. Shown in (A) is the superposition of the four orientations of the right-hand side of **14** in the bound state that are consistent with the ensemble of transferred NOESY partially displayed in (B)-(D). The methods employed for determining these structures are similar to those described in reference 3. Compounds **15** and **16** are purified enantiomers (the exact stereochemistry is undetermined).

Collectively, the data suggested that one may not deduce a single accurate bound conformation that would be representative of this series. A more appropriate approach would be to consider that the right-hand sides may adopt multiple possible orientations which lie flat onto the upper plateau of the receptor. The transferred NOESY data indicated that these conformations were due mainly to differences in the ζ and ε torsion angles with significant interdependence on δ. These multiple orientations were modeled using compound **14** for convenience and taking into account the above differences noted for compounds **14**, **15** and **16**. Four complementary flat conformations involving torsion angles ζ and ε were modeled for compound **14** as shown in Figure 6A. These binding modes are consistent with our extensive structure-activity studies where it was found that

a variety of substituents were tolerated and complemented the flat surface feature of the upper plateau of the receptor (data not shown). For example, Appendix 3 of the Supporting Information shows a series of substituents meta, para or ortho to the aniline nitrogen to probe the spacial range that was tolerated. Although all compounds maintained flat conformations in the free-state, the para and meta substituents exhibited similar potencies whereas the ortho substituent resulted in a loss in activity (also noted for other unpublished examples). Thus, it became apparent that many substitutions were tolerated as long as planarity was maintained where the flat ligand conformations properly complemented the available surface feature of the upper plateau.

The ensemble of conformations shown in Figure 6A suggested that conformationally rigidified bioisosteres of the right-hand side amide moiety may be acceptable replacements. Bioisosteres of amide bonds are of significant utility in drug design as they often lead to compounds with improved cell-based potency and physicochemical properties.[11] The most fruitful of our approaches is illustrated in Figure 7. The amide-aryl segment of the monocyclic diamide series **4** was replaced by a benzimidazole moiety in order to eliminate the amide bond and restrict rotation along ζ. Although multiple types of bioisosteres were tolerated (data not shown), the structural modification shown in Figure 7 ultimately led to the discovery of deleobuvir (BI 207127) (compound **17**) which is currently in phase III clinical trials.[10]

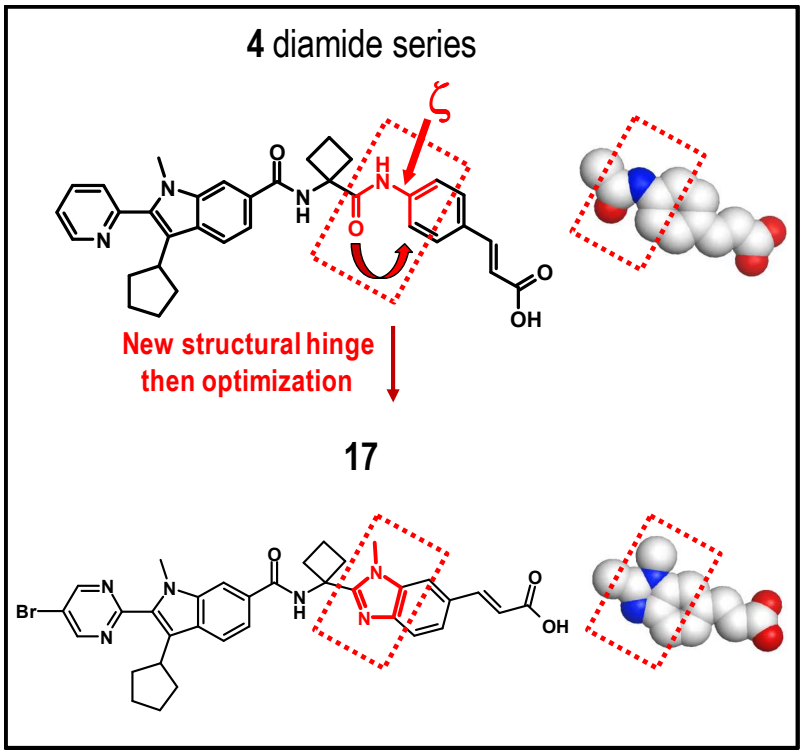

Figure 7. Redesign of the structural hinge leading from diamide **4** to **17**.

Figure 8B shows a model of **17** bound to the thumb pocket I subdomain of HCV polymerase. A close-up view given in Figures 8C reveals details of the binding mode where the red dotted box highlights the cyclized ring discussed above which lies flat on the upper plateau of the receptor. The colored surfaces in Figure 8C highlight the position of amino acid substitutions associated with compound resistance that lie immediately below the new right-side appendage that provided biological corroboration of this binding site.[7e]

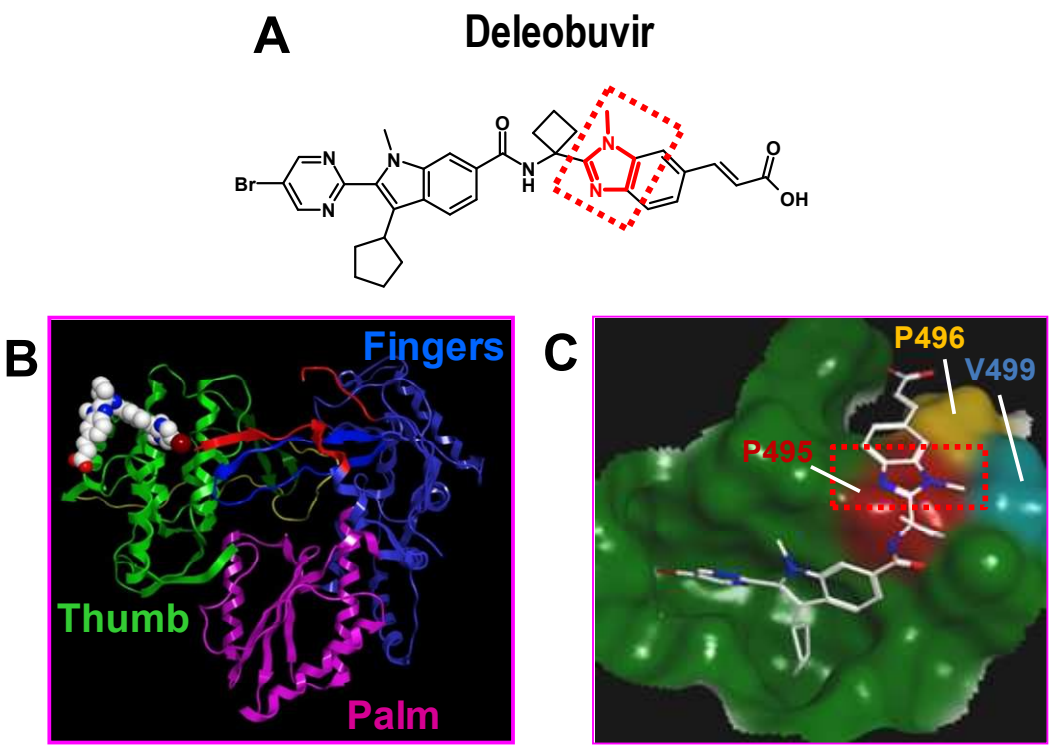

Figure 8. (A) The structure of deleobuvir (**17**) is shown with a red-dotted box that highlights the region implicated in the novel structural hinge. (B) The space-filling view of **17** is displayed when docked to NS5B based on the X-ray structures of the apo and a related complex as described in detail earlier (PDB accession codes for the latter are 3MWV and 3MWW).[3] (C) Stick view of **17** in the thumb I binding pocket.

Compound **17** is a potent and specific inhibitor of GT-1 HCV polymerase activity (IC_{50} = 50 nM) and subgenomic antiviral activity (EC_{50} = 11 nM and 23 nM in cell-based replicon GT1b and GT1a assays), and shows weak or no inhibition in specificity assays that include poliovirus RdRp, mammalian DdRp II and DNA polymerase α, β, and γ.[10,12] Furthermore, its *in vitro* ADME and *in vivo* cross-species PK profiles are consistent with further progression into drug development.[14] Compound **17** displayed good antiviral potency and tolerability in early clinical trials of short-term treatment either as a single agent or in combination with pegylated interferon-*a*2a/ribavirin (RBV) in HCV GT1 patients.[8d] Moreover, the IFN-free combination of our NS3 protease inhibitor faldaprevir

in combination with **17** and RBV has demonstrated high efficacy and good tolerability in GT1b treatment-naive patients in phase II clinical trials.[10]

CONCLUSIONS

This work presents examples of how NMR-guided conformational restrictions and scaffold replacements are valuable strategies in drug design. Knowledge building via structure and dynamics approaches was found to be critical for hypotheses generation and follow-up studies. Here, we reported examples where promising new chemotypes were discovered and a new series led to a compound that advanced to clinical development.

MATERIALS AND METHODS

HCV assays. Inhibition of GT-1b HCV NS5BΔ21 enzymatic activity was performed as previously described.[7g] The bicistronic luciferase reporter replicon, encoding the Con1 GT-1b NS2-NS5B coding region, and the experimental procedures for measuring EC_{50} values in the experiments reported above have been described elsewhere.[12] Compounds were incubated with cells for 72 hours and the relative levels of luciferase present were determined using the Bright-Glo luciferase substrate (Promega) on a Packard Topcount instrument. Alternatively, GT-1a or GT-1b HCV subgenomic stable cell lines (129-S.16 or S22.3 cells, respectively) established at the Boehringer Ingelheim (Canada) Ltd R&D labs were also used to assess inhibition of HCV RNA replication in cell culture through quantification of HCV RNA levels by TaqMan quantitative real-time RT-PCR.[7e] EC_{50} values were determined by the non-linear

regression routine NLIN procedure of SAS (EC_{50}). All reported values are the average of at least ≥2 measurements.

Bound structures based on X-ray, NMR and docking. The data presented in this work employed the same constructs, enzymatic assay and cell-culture assay as reported previously.[3] The bound structures of compounds **4**, **17** and **14-16** were determined using a combination of X-ray, NMR and docking as described elsewhere.[3] Overall, they were docked to NS5B based on the X-ray structures of the apo and a related complex as described in detail earlier (PDB accession codes for the latter are 3MWV and 3MWW).[3]

NMR transferred NOESY data: NOESY data were collected to extract intramolecular hydrogen distances of compounds **14-16** and **S3** when bound to HCV polymerase. These distances were then applied as constraints in simulated annealing calculations to identify low-energy structures that also satisfy the NMR constraints. All of the compounds were soluble in buffer at concentrations equal to or greater than 0.2 mM, showed no evidence of self-aggregation as determined by NOESY and/or DLS data, had equal to or longer stability than 24 hours when in complex with HCV polymerase, and had relatively low levels of spin-diffusion artifacts.

For each compound, a multitude of transferred NOESY data were collected using many samples on 400, 600, and 800 MHz NMR spectrometers. NOESY data were processed using XWIN-NMR and Win2D software, and the NOESY crosspeaks were completely assigned by applying a combination of ROESY, COSY, NOESY, 1D spectra, HMQC, and HMBC data. Volumes of NOESY crosspeaks were measured and translated to inter-hydrogen distances. The 3D structures were calculated using MSI or CCG

modeling software. A protocol which is similar to that previously described by LaPlante *et al., J. Biol. Chem.* 274, 18618-18624 (1998) was applied.

ASSOCIATED CONTENT

Supporting Information

Supporting Information section is available that describes materials & methods and other relevant experiments. A synthesis procedure for compound **17** is also provided. This material is available free of charge via the Internet at http://pubs.acs.org.

AUTHOR INFORMATION

Corresponding Information

*Adress all correspondence to RESGeneral.LAV@boehringer-ingelheim.com

‡ Curent adresses: For SRL, NMX Solutions, 500 boulevard Cartier Ouest, Suite 6000, Laval, Qc, Canada H7V 5B7, e-mail: stevenrlaplante@gmail.com; for YST, Department of Chemistry, McGill University, 801 Sherbrooke Street West, Montreal, QC, Canada H3A 0B8, e-mail: youla.tsantrizos@mcgill.ca

ACKNOWLEDGEMENTS

We are grateful to the following colleagues: P. Anderson, N. Aubry, R. Bethell, D. Cameron, M. Cordingley, J.-M. Ferland, M.-A. Poupart and F. Stasi. We also acknowledge the valuable teamwork and contributions of our colleagues at Boehringer Ingelheim.

ABBREVIATIONS USED

ADME, absorption, delivery, metabolism, excretion; clogP, calculated partition coefficient; DdRP, DNA-dependent RNA polymerase; DLB, differential line broadening; DMSO, dimethyl sulphoxide; HCV, hepatitis C virus; HPLC, high-pressure liquid chromatography; HTS, high-throughput screen; IFN, interferon; NMR, nuclear magnetic resonance; NOESY, nuclear Overhauser exchange spectroscopy; NS3, non-structural HCV protease; RBV, ribavirin; RdRp, RNA-dependent RNA polymerase; ROESY, rotating-frame exchange spectroscopy; SAR, structure-activity relationship.

REFERENCES

(1) a) Teague, S. Implications of protein flexibility for drug discovery. *Nature Rev. Drug Disc.* **2003**, *2*, 527-541; b) Weikl, T.R.; von Deuster, C. Selected-fit versus induced-fit protein binding: Kinetic differences and mutational analysis. *Proteins: Structure, Function, and Bioinformatics* **2009**, *75*, 104-110; c) Hammes, G.G.; Chang, Y.C.; Oas, T.G. Conformational selection or induced fit: A flux description of reaction mechanism. *Proc. Nat. Acad. Sci. USA* **2009**, *106*, 13737-13741; d) Bakan, A.; Bahar, I. The intrinsic dynamics of enzymes plays a dominant role in determining the structural changes induced upon inhibitor binding. *Proc. Nat. Acad. Sci. USA* **2009**, *106*, 14349-14354; e) Lakomek, N.A.; Lange, O.F.; Oliver, F.; Walter, K.F.; Korvin, F.A.; Fares, C.; Egger, D.; Lunkenheimer, P.; Meiler, J.; Grubmueller, H.; Becker, S.; de Groot, B.L.; Griesinger, C. Residual dipolar couplings as a tool to study molecular recognition of ubiquitin. *Biochem. Soc. T.* **2008**, *36*, 1433-1437; f) Lange, O.F.; Lakomek, N.A.; Fares, C.; Schroeder, G.F.; Gunnar, G.; Walter, K.F.A.; Becker, S.; Meiler, J.; Grubmueller, H.;

Griesinger, C.; de Groot, B.L. Recognition dynamics up to microseconds revealed from an RDC-derived ubiquitin ensemble in solution. *Science* **2008**, *320*, 1471-1475. g) Kern, D.; Zuiderweg, E.R. The role of dynamics in allosteric regulation. *Curr. Opin. Struct. Biol.* **2003**, *13*, 748-757; f) Mittermaier, A.; Kay, L.E. New tools provide new insights in NMR studies of protein dynamics. *Science* **2006**, *312*, 224-228.

(2). Koshland, D. The active site and enzyme action. *Adv. Enzymol. Relat. Subj. Biochem.* **1960**, *22*, 45-97.

(3) LaPlante, S.R.; Gillard, J.R.; Jakalian, A.; Aubry, N.; Coulombe, R.; Brochu, C.; Tsantrizos, Y.S.; Poirier, M.; Kukolj, G.; Beaulieu, P.L. Importance of ligand bioactive conformation in the discovery of potent indole-diamide inhibitors of the hepatitis C virus NS5B. *J. Am. Chem. Soc.* **2010***, 132*, 15204-15212.

(4) a) Peng, J.W. New probes of ligand flexibility in drug design: transferred (13)C CSA-dipolar cross-correlated relaxation at natural abundance. *J. Am. Chem. Soc.* **2003**, *125*, 11116-11130; b) LaPlante, S.R.; Aubry, N.; Déziel, R.; Ni, F.; Xu, P. Transferred 13C T1 relaxation at natural isotopic abundance: A practical method for determining site-specific changes in ligand flexibility upon binding to a macromolecule. *J. Am. Chem. Soc.* **2000**, *122*, 12530-12535; c) Peng, W.; Wilson, B.D.; Namanja, A.T. Mapping the dynamics of ligand reorganization via $^{13}CH_3$ and $^{13}CH_2$ relaxation dispersion at natural abundance. *J. Biomolecular NMR* **2009**, *45,* 1-2, 171-183; d) Peng, J.W. Communication Breakdown: Protein dynamics and drug design. *Structure* **2009**, *17*, 319-320; e) Mauldin, R.V.; Carroll, M.J.; Lee, A.L. Dynamic dysfunction in dihydrofolate reductase results from antifolate drug binding: Modulation of dynamics within a structural state. *Structure* **2009**, *17*, 386-394; f) Taylor, R.E.; Chen, Y.; Beatty, A; Myles, D.C.; Zhou, Y.

Conformation−Activity Relationships in polyketide natural products: A new perspective on the rational design of epothilone analogues *J. Am. Chem. Soc.*, **2003**, *125*, 26–27; g) Thoma, G.; Magnani, J.L.; Patton, J.T.; Ernst, B.; Jahnke, W. Preorganization of the bioactive conformation of sialyl Lewis^X analogues correlates with their affinity to E-selectin. *Angew. Chem. Int. Ed.* **2001**, *125*, 1941-1945.

(5) a) Kramer, B.; Rarey, M.; Lengauer, T. Evaluation of the FLEXX incremental construction algorithm for protein-ligand docking. *Proteins* **1999**, *37*, 228-241; b) Verdonk, M.L.; Cole, J.C.; Hartshorn, M.J.; Murray, C.W.; Taylor, R.D. Improved protein-ligand docking using GOLD. *Proteins* **2003**, *52*, 609-623; c) Goodsell, D.S. Computational docking of biomolecular complexes with AutoDock *CSH Protoc* **2009**, 2009 (pdb prot5200); d) Morris, G.M.; Huey, R.; Olson, A.J. Using AutoDock for ligand-receptor docking. *Curr Protoc Bioinformatics* **2008**, chapter 8, unit 814; e) Ewing, T.J.; Makino, S.; Skillman, A.G.; Kuntz, I.D. DOCK 4.0: Search strategies for automated molecular docking of flexible molecule databases. *J. Comput. Aided Mol. Des.* **2001**, *15*, 411-428; f) McGann, M.R.; Almond, H.R.; Nicholls, A.; Grant, J.A.; Brown, F.K. Gaussian docking functions. *Biopolymers* **2003**, *68*, 76-90; g) Goto, J.; Kataoka, R.; Muta, H.; Hirayama, N. ASEDock-docking based on alpha spheres and excluded volumes. *J. Chem. Inf. Model.* **2008**, *48*, 583-590; h) Tondel, K.; Anderssen, E.; Drablos, F. Protein Alpha Shape (PAS) Dock: A new gaussian-based score function suitable for docking in homology modeled protein structures. *J. Comp. Aided Mol. Des.* **2006**, *20*, 131-144. i) Jackson, S.; DeGrado, W.; Dwivedi, A.; Parthasarathy, A.; Higley, A.; Krywko, J.; Rockwell, A.; Markwalder, J.; Wells, G. Template-constrained cyclic peptides: Design of high-affinity ligands for GPIIb/IIIa. *J. Am. Chem. Soc.* **1994**, *116*,

3220-3230; j) Miller, C.P.; Collini, M.D.; Harris, H.A. Constrained phytoestrogens and analogues as ERbeta selective ligands. *Bioorg. Med. Chem. Lett.* **2003**, *13*, 2399-2403; k) Udugamasooriya, D.G.; Spaller, M.R. Conformational constraint in protein ligand design and the inconsistency of binding entropy *Biopolymers*, **2008**, *89*, 653-667; l) Sharma, R.; Lee, J.; Wang, S.; Milne, G.W.A.; Lewin, N.E.; Blumberg, P.M.; Marquez, V.E. Conformationally constrained analogues of diacylglycerol. 10. Ultrapotent protein kinase C ligands based on a racemic 5-disubstituted tetrahydro-2-furanone template. *J. Med. Chem.* **1996**, *39*, 19-28; m) Martin, S.F. Preorganization in biological systems: Are conformational constraints worth the energy? *Pure Appl. Chem*. **2007**, *79*, 193–200; n) Harris, P.W.R.; Hügel, H.M.; Nurlawis, F. A review of the molecular conformations of melatonin ligands at the melatonin receptor. *Molecular Simulation* **2002**, *28*, 889-902; o) Giebel, L.B.; Cass, R.; Milligan, D.L.; Young, D.; Arze, R.; Johnson, C. Screening of cyclic peptide phage libraries identifies ligands that bind streptavidin with high affinities. *Biochemistry* **1995**, *34*, 15430-15435.

(6) a) Choo, Q.-L.; Kuo, G.; Weiner, A. J.; Overby, L. R.; Bradley, D. W.; Houghton, M. Isolation of a cDNA clone derived from a blood-borne non-A, non-B viral hepatitis genome. *Science* **1989**, *244*, 359-362; b) Lavanchy, D. The global burden of hepatitis C. *Liver Int*. **2009**, *29*, 74-81; c) O'Brien, C.; Godofsky, E.; Rodriguez-Torres, M.; Afdhal, N.; Pappas, S. C.; Pockros, P.; Lawitz, E.; Bzowej, N.; Rustgi, V.; Sulkowski, M.; Sherman, K.; Jacobson, I.; Chao, G.; Knox, S.; Pietropaolo, K.; Brown, N. A. Randomized trial of valopicitabine (NM283), alone or with peg-interferon, vs. retreatment with peg-interferon plus ribavirin (pegIFN/RBV) in hepatitis C patients with previous non-response to PegIFN/RBV: first interim results. *Hepatology* **2005**, *42*, 234A;

d) Brown, N. Progress towards improving antiviral therapy for hepatitis C with hepatitis C virus polymerase inhibitors. Part I: Nucleoside analogues. *Expert. Opin. Invest. Drugs* **2009**, *18*, 709-725; e) Huang, Z.; Murray, M. G.; Secrist, J. A., III Recent development of therapeutics for chronic HCV infection. *Antiviral Res.* **2006**, *71*, 351-362.

(7) a) Beaulieu, P. L.; Bös, M.; Bousquet, Y.; Fazal, G.; Gauthier, J.; Gillard, J.; Goulet, S.; LaPlante, S.L.; Poupart, M.A.; Lefebvre, S.; McKercher, G.; Pellerin, C.; Austel, V.; Kukolj, G. Non-nucleoside inhibitors of the hepatitis C virus NS5B polymerase: discovery and preliminary SAR of benzimidazole derivatives. *Bioorg. Med. Chem. Lett.* **2004**, *14*, 119-124; b) Beaulieu, P.L.; Bös, M.; Bousquet, Y.; DeRoy, P.; Fazal, G.; Gauthier, J.; Gillard, J.; Goulet, S.; Poupart, M.-A.; Valois, S.; McKercher, G.; Kukolj, G. Non-nucleoside inhibitors of the hepatitis C virus NS5B polymerase: discovery of benzimidazole 5-carboxylic amide derivatives with low-nanomolar potency. *Bioorg. Med. Chem. Lett.* **2004**, *14*, 967-971; c) Beaulieu, P.L.; Gillard, J.; Bykowski, D.; Brochu, C.; Dansereau, N.; Duceppe, J.S.; Haché, B.; Jakalian, A.; Lagacé, L.; LaPlante, S.R.; McKercher, G.; Moreau, E.; Perreault, S.; Stammers, T.; Thauvette, L.; Warrington, J.; Kukolj, G. Improved replicon cellular activity of non-nucleoside allosteric inhibitors of HCV NS5B polymerase: from benzimidazole to indole scaffolds. *Bioorg. Med. Chem. Lett.* **2006**, *16*, 4987-4993; d) Beaulieu, P.L.; Bousquet, Y.; Gauthier, J.; Gillard, J.; Marquis, M.; McKercher, G.; Pellerin, C.; Valois, S.; Kukolj, G. Non-nucleoside benzimidazole-based allosteric inhibitors of the hepatitis C virus NS5B polymerase: inhibition of subgenomic hepatitis C virus RNA replicons in Huh-7 cells. *J. Med. Chem*. **2004**, *47*, 6884-6892; e) Kukolj, G.; McGibbon, G.; McKercher, G.; Marquis, M.; Lefebvre, S.; Thauvette, L.; Gauthier, J.; Goulet, S.; Poupart, M.A.; Beaulieu, P.L.

Binding site characterization and resistance to a class of non-nucleoside inhibitors of the hepatitis C virus NS5B polymerase. *J. Biol. Chem.,* **2005**, *280*, 39260-39267; f) Goulet, S.; Poupart, M.A.; Gillard, J.; Poirier, M.; Kukolj, G.; Beaulieu, P.L. Discovery of benzimidazole-diamide finger loop (Thumb Pocket I) allosteric inhibitors of HCV NS5B polymerase: Implementing parallel synthesis for rapid linker optimization. *Bioorg. Med. Chem. Lett.* **2010**, *20*, 196-200; g) McKercher, G.; Beaulieu, P.L.; Lamarre, D.; LaPlante, S.R.; LeFebvre, S.; Pellerin, C.; Thauvette, L.; Kukolj, G. Specific inhibitors of HCV polymerase identified using an NS5B with lower affinity for template/primer substrate. *Nucleic Acids Research,* **2004**, *32*, 422-431. h) LaPlante, S.R.; Jakalian, A.; Aubry, N.; Bousquet, Y.; Ferland, J.M.; Gillard, J.; Lefebvre, S.; Poirier, M.; Tsantrizos, Y.S.; Kukolj, G.; Beaulieu, P.L. Binding mode determination of benzimidazole inhibitors of the hepatitis C virus RNA polymerase by a structure and dynamics strategy. *Angew. Chem. Int. Ed.* **2004**, *43*, 4306-4311.

(8) a) Beaulieu, P.L.; Bös, M.; Cordingley, M.G.; Chabot, C.; Fazal, G.; Garneau, M., Gillard, J.R.; Jolicoeur, E.; LaPlante, S.; McKercher, G.; Poirier, M.; Poupart, M-A.; Tsantrizos, Y.S.; Duan, J.; Kukolj, G. Discovery of the First Thumb Pocket 1 NS5B polymerase inhibitor (BILB 1941) with demonstrated antiviral activity in patients chronically infected with genotype 1 hepatitis C virus (HCV). *J. Med. Chem.* **2012**, *55*, 7650-7666. b) Erhardt, A.; Deterding, K.; Benhamou, Y.; Reiser, M.; Forns, X.; Pol, S.; Calleja, J.L.; Ross, S.; Spangenberg, H.C.; Garcia-Samaniego, J.; Fuchs, M.; Enriquez, J.; Wiegand, J.; Stern, J.; Wu, K.; Kukolj, G.; Marquis, M.; Beaulieu, P.; Nehmiz, G.; Steffgen, J. Safety, pharmacokinetics and antiviral effect of BILB 1941, a novel hepatitis C virus RNA polymerase inhibitor, after 5 days oral treatment. *Antiviral Therapy*, **2009**,

14, 23-32. c) Beaulieu, P.L. Recent advances in the development of NS5B polymerase inhibitors for the treatment of hepatitis C virus infection. *Expert Opin. Ther. Pat.*, **2009**, *19*, 145-164. d) Beaulieu, P.L. RSC Drug Discovery Series No. 32, Successful strategies for the discovery of antiviral drugs. Eds. M. Desai, N. Meanwell, The Royal Society of Chemistry **2013**, Chapter 9, 279.

(9) a) Ikegashira, K.; Oka, T.; Hirashima, S.; Noji, S.; Yamanaka, H.; Hara, Y.; Adachi, T.; Tsuruha, J.-I.; Doi, S.; Hase, Y.; Noguchi, T.; Ando, I.; Ogura, N.; Ikeda S.; Hashimoto, H. Discovery of conformationally constrained tetracyclic compounds as potent hepatitis C virus NS5B RNA polymerase inhibitors. *J. Med. Chem.*, **2006**, 6950-6953. b) Stanfield, I.; Ercolani, C.; Mackay, A.; Conte, I.; Pompei, M.; Koch, U.; Gennari, N.; Giuliano, C.; Rowley M.; Narjes, F. Tetracyclic indole inhibitors of hepatitis C virus NS5B-polymerase. *Bioorg. Med. Chem. Lett.,* **2009**, *19*, 627-632. c) Habermann, J.; Capito, E.; del Rosario Rico, M.; Ferreira, U.; Koch, U.; Narjes, F. Discovery of pentacyclic compounds as potent inhibitors of hepatitis C virus NS5B RNA polymerase. *Bioorg. Med. Chem. Lett.,* **2009**, *19*, 633-638. d) Ding, M.; He, F.; Hudyma, T.W.; Zheng, X.; Poss, M.A.; Kadow, J.F.; Beno, B.R.; Rigat, K.L.; Wang, Y.K.; Fridell, R.A.; Lemm, J.A.; Qiu, D.; Liu, M.; Voss, S.; Pelosi, L.A.; Roberts, S.B.; Gao, M.; Knipe, J.; Gentles, R. Synthesis and SAR studies of novel heteroaryl fused tetracyclic indole-diamide compounds: Potent allosteric inhibitors of the hepatitis C virus NS5B polymerase. *Bioorg. Med. Chem. Lett.,* **2012**, *22*, 2866-2871. e) Vendeville, S.; Lin, T.-I.; Hu, L.; Tahri, A.; McGowan, D.; Cummings, D.; Amssoms, K.; Canard, M.; Last, S.; van den Steen, I.; Devogelaere, B.; Rouan, M.-C.; Vijgen, L.; Berke, J.M.; Dehertogh, P.; Fransen, E.; Cleiren, E.; van der Helm, L.; Fanning, G.; van Emelen, K.; Nyanguile, O.;

Simmen K.; Raboisson, P. Finger loop inhibitors of the HCV NS5b polymerase. Part II. Optimization of tetracyclic indole-based macrocycle leading to the discovery of TMC647055. *Bioorg. Med. Chem. Lett.,* **2012**, *22*, 4437-4443. f) Cummings, M.D.; Lin, T.-I.; Hu, L.; Tahri, A.; McGowan, D.; Amssoms, K.; Last, S.; Devogelaere, B.; Rouan, M.-C.; Vijgen, L.; Berke, J.M.; Dehertogh, P.; Fransen, E.; Cleiren, E.; van der Helm, L.; Fanning, G.; van Emelen, K.; Nyanguile, O.; Simmen, K.; Raboisson P.; Vendeville, S. Structure-based macrocyclization yields hepatitis C virus NS5B inhibitors with improved binding affinities and pharmacokinetic properties. *Angew. Chem. Int. Ed.,* **2012***, 51,* 4637-4640.

(10) a) Larry, D.; Benhamou, Y., ; Lohse, A.W.; Trepo, C.; Moelleken, C.; Bronowicki, J.-P.; Arasteh, K.; Bourliere, M.; Heim, M.; Enrıquez, J., Erhardt, A.; Zarski, J.P.; Wiest, R.; Gerlach, T.; Wedemeyer, H., Berg, T.; Stern, J.; Wu, K., Abdallah, N.; Nehmiz, G.; Boecher, W.; Steffgen, J. Safety , Pharmacokinetics and antiviral effect of BI 207127, a novel HCV RNA polymerase inhibitor, after 5 days oral treatment in patients with chronic hepatitis C. *J. Hepatol.*, **2009**, *50* (Suppl. 1)*, S383-S384*, Abstract 1054; b) Zeuzem, S.; Asselah, S.; Angus, P.; Zarski, J.-P.; Larrey, D.; Mullhaupt, H.; Gane, E.; Schuchmann, M.; Lohse, A.; Pol, S.; Bronowicki, J.-P,; Roberts, S.; Arasteth, A.; Zoulim, A.; Heim, M.; Stern, J.O.; Kukolj, G.; Nehmiz, H.; Haefner, C.; Boecher, W.O., Efficacy of the protease inhibitor BI 201335, polymerase inhibitor BI 207127, and ribavirin in patients with chronic HCV infection. *Gastroenterology*, **2011**, *141*, 2047-2055; c) Zeuzem, S.; Soriano, V.; Asselah, T.; Bronowicki, J.-P.; Lohse, A.; Müllhaupt, B.; Schuchmann, M.; Bourliere, M.; Buti, M.; Roberts, S.; Gane, E.; Stern, J.O.; Kukolj, G.; Dai, L.; Böcher, W.O.; Mensa, F.J., SVR4 and SVR12 with an interferon-free regimen of

BI201335 AND BI207127, +/- ribavirin, in treatment-naive patients with chronic genotype-1 HCV infection: Interim results of SOUND-C2, *J. Hepatol*., **2012**, *56*, Suppl. 2, S45; d) Zeuzem, S.; Soriano, V.; Asselah, T.; Bronowicki, J.-P.; Lohse, A.W.; Müllhaupt, B.; Schuchmann, M.; Bourlière, M.; Buti, M.; Roberts, S.K.; Gane, E.J.; Stern, J.O.; Vinisko, R.; Kukolj, G.; Gallivan, J.-P.; Böcher, W.-O.; Mensa, F.J., Faldaprevir and deleobuvir for HCV genotype 1 infection. *N. Engl. J. Med.* **2013**, *369*, 630-639.

(11) Meanwell, N.A. Synopsis of some recent tactical application of bioisosteres in drug design. *J. Med. Chem*. **2011**, *54*, 2529-2591.

(12) a) Vaillancourt, F. H.; Pilote, L.; Cartier, M.; Lippens, J.; Liuzzi, M.; Bethell, R. C.; Cordingley, M. G.; Kukolj, G. Identification of a lipid kinase as a host factor involved in hepatitis C virus RNA replication. *Virology* **2009**, *387*, 5-10. b) Beaulieu, P.L.; Fazal, G.; Goulet, S.; Kukolj, G.; Piorier, M.; Tsantrizos, Y., Jolicoeur, E.; Gillard, J.; Poupart, M.-A.; Rancourt, J. Viral Polymerase Inhibitors, Patent WO 03/010141, **2003**.

(13) LaPlante, S.R.; Aubry, N.; Bonneau, P.; Kukolj, G.; Lamarre, D.; Lefebvre, S.; Li, H.; Llinàs-Brunet, M.; Plouffe, C.; Cameron, D.R. NMR line-broadening and transferred NOESY as a medicinal chemistry tool for studying inhibitors of the hepatitis C virus NS3 protease domain, *Bioorg. Med. Chem. Lett.* **2000**,*10*, 2271-2274.

(14) a) Beaulieu, P.L.; Anderson, P.C.; Bös, M.; Brochu, C.; Cordingley, M.G.; Duan, J.; Garneau, M.; Lagacé, L.; LaPlante, S.R.; Marquis, M.; McKercher, G.; Poupart, M.-A.; Rancourt, J.; Stammers, T.; Tsantrizos, Y.S.; Kukolj, G. Preclinical characterization of the hepatitis C virus NS5B polymerase non-nucleoside inhibitor BI 207127. 19th International Symposium on Hepatitis C Virus and Related Viruses, 5-9 October **2012**,

Venice, Italy; b) Duan, J.; Bolger, G.; Garneau, M.; Amad, M.; Batonga, J.; Montpetit, H.; Otis, F.; Jutras, M.; Lapeyre, N.; Rhéaume, M.; Kukolj, G.; White, P.W.; Bethell, R.C.; Cordingley, M.G. The liver partition coefficient-corrected inhibitory quotient and the pharmacokinetic-pharmacodynamic relationship of directly acting anti-hepatitis C virus agents in humans. *Antimicrob. Agents Chemother.,* **2012** ; *56*, 5381-5386.

TABLE OF CONTENTS GRAPHIC